

# Distributed Adaptive Virtual Impedance Control for Power Sharing in an Islanded Microgrid

Manoj Dahal

*Department of Electrical Engineering  
National Institute of Technology  
Warangal, India  
md22eem3r08@student.nitw.ac.in*

Ram Krishan, Senior Member, IEEE

*Department of Electric Engineering  
National Institute of Technology  
warangal, India  
rkrishan@nitw.ac.in*

**Abstract**—Accurate active and reactive power sharing in islanded microgrids is a prominent challenge. The existing conventional droop control strategies for power-sharing have disadvantages like inaccurate power-sharing among distributed generators (DGs) in the case of feeder impedance mismatch, unequal ratings of the sources etc. The complexity intensifies in the case of reactive power sharing. Virtual impedance emerges as a widely adopted technique to address impedance mismatches; however, the key challenge lies in determining the optimal value for its configuration. This paper proposes an adaptive virtual output impedance-based control for proportionate sharing of powers among the parallel connected DGs in the microgrid. The proposed control method is evaluated with the information of neighbouring DGs with data integrity. The primary focus of the paper is to attain accurate reactive power sharing. A small signal stability analysis of the system is carried out to ensure its performance. Various case studies are simulated in MATLAB Simulink to validate the robustness of the proposed control strategy.

**Index Terms**—Virtual impedance, Adaptive control, Reactive power, Consensus, Communication delay

## I. INTRODUCTION

The increased integration of Renewable Energy Sources (RESs) has exposed conventional power systems to heightened vulnerability, leading to stability and reliability challenges. A transformative shift has emerged with the advent of microgrids, presenting a promising opportunity to seamlessly incorporate RESs into the grid, thereby revolutionising the conventional power system paradigm [1]. Moreover, a microgrid also has its own challenges, especially in the case of its islanded operation. Various stability problems arise due to unequal voltage drop, power-sharing ratios, etc. [2]. The power-sharing problems in parallel connected DGs have drawn the attention of researchers in recent years. As the voltage and frequency droop of an inverter-based microgrid is directly related to reactive and active power shared, various droop-based techniques are proposed. Hierarchical control strategies (primary, secondary and tertiary level controls) are being adopted in microgrids by learning from conventional plants [3]–[5]. One of the problems with hierarchical control is communication disruption and delay among the levels of control. Droop control comes under the primary level control

and, if implemented alone, then avoids the communication-related problem. However, this comes at the cost of deviating voltage and frequency from their nominal values. Conventional droop control leads to poor reactive power sharing in case of line impedance mismatch and differences in ratings of the distributed generators. Also, due to the low  $X/R$  ratio in a microgrid, the assumption considering the line impedance as predominantly inductive in conventional control becomes wrong. There are various improved droop control techniques proposed in [6]–[8] to overcome the power-sharing problem in conventional techniques. The droop control strategy discussed in [9] has poor performance if there is a lossy network. Primary control leads to voltage and frequency control, and as a part of hierarchical control, secondary control is implemented [10], [11]. Further, secondary control can be both centralized and decentralized. The decentralized control techniques help in avoiding communication delay-related issues [12], [13]. In such cases, controller-to-controller synchronization is a tedious task. Apart from communication delay, the focus has been there to minimize the circulating current. Reference [14] describes the method for decoupling among the line impedances and reactive power and proposes methods to achieve minimum circulating current. But increase in resistive elements may still lead to active and reactive power coupling, thereby leading to problems in independent control. Instead of improved droop control techniques, virtual impedance techniques are also used for power sharing [15], [16]. The virtual output impedance technique can be only resistance-based, reactance-based, or duel impedance-based. A duel impedance-based adaptive virtual output impedance technique is proposed in [17], but the voltage drop issue is not addressed.

In this paper, an adaptive virtual output impedance control method for proportionate power sharing is implemented along with a consensus-based voltage restoration technique to obtain the desired value of average output voltage. A consensus-based algorithm is applied to get information about the individual reactive power from each DGs. This information helps to generate the reactive power mismatch value, and based on this reactive power mismatch value, the virtual impedance correction term is obtained, and the virtual impedance is updated accordingly. As virtual impedance may lead to voltage drop, a voltage restoration technique is used to restore the

This research was supported by the Science and Engineering Research Board (SERB) DST India under grant number SRG/2021/000810.

voltage to its desired average value.

The rest of the paper is organized as follows: Section II talks about conventional droop control, while the proposed controller is discussed in section III. Section IV gives the idea of preliminary graph theory, discusses the adaptive virtual impedance control based on consensus algorithm and shows the modification in reference value of voltage due to the effect of virtual impedance. Section V shows the simulation result of the proposed model considering various cases. Small signal stability of the proposed model considering the effect of virtual impedance is described in section VI. Section VII concludes the paper.

## II. CONVENTIONAL DROOP CONTROL

Generally, conventional droop controllers are designed with the measured output voltages ( $V$ ) and currents ( $I$ ) obtained in the  $dq0$  reference frame. Using measured  $V$  and  $I$ , the instantaneous values of active and reactive powers can be written as

$$p = \frac{3}{2} (v_{od} i_{od} + v_{oq} i_{oq}) \quad (1)$$

$$q = \frac{3}{2} (v_{od} i_{oq} - v_{oq} i_{od}) \quad (2)$$

After passing through low pass filter in order to avoid the oscillations and eventually the average active and reactive power modifies to

$$P = \frac{\omega_c}{s + \omega_c} p \quad (3)$$

$$Q = \frac{\omega_c}{s + \omega_c} q \quad (4)$$

Where  $\omega_c$  is the cut-off frequency for the low pass filter. The conventional droop control equations are

$$\omega = \omega_n - mP \quad (5)$$

$$V_{oi} = V_n - nQ \quad (6)$$

Now the  $d$  and  $q$  component of voltage references are given by

$$v_{od}^* = V_n - nQ \quad (7)$$

$$v_{oq}^* = 0 \quad (8)$$

Where  $m$  and  $n$  are active and reactive power droop coefficients respectively. The conventional control gives satisfactory results only for the active power sharing but not for reactive power sharing in case of mismatched line impedances. Proposed controller leads to proportionate sharing of reactive power sharing irrespective of the line impedances values.

## III. PROPOSED CONTROLLER

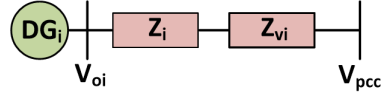


Fig. 1. DG connected to common AC bus through line impedance.

In conventional droop control we assume the network is more inductive in nature which is not true in case of microgrid where the  $X/R$  ratio is low. In this proposed control the introduction of virtual impedance leads to improved  $X/R$  ratio facilitating the power sharing control. Considering Fig.1, the reactive power output from DG injected to bus  $i$  without considering virtual impedance can be expressed as:

$$Q_i = \left( \frac{V_{oi} V_{PCC}}{Z_i} \cos \phi_i - \frac{V_{PCC}^2}{Z_i} \right) \sin \theta_i - \frac{V_{oi} V_{PCC}}{Z_i} \sin \phi_i \cos \theta_i \quad (9)$$

Assuming negligibly small power angle  $\phi_i$  and considering the microgrid eventually becomes more inductive leading to an improved  $X/R$  ratio after the addition of virtual impedance  $Z_{vi}$ ; the above equation modifies to:

$$Q_i = \frac{V_{pcc} (V_{oi} - V_{pcc})}{(X_i + X_{vi})} \quad (10)$$

Where  $X_i$  is line reactance while  $X_{vi}$  is the virtual reactance value.  $X_{vi}$  consists of two components, static and adaptive components. The adaptive component value keeps on changing based on the reactive power mismatch. Substituting (6) in (10) we get

$$n_i Q_i = \frac{V_{pcc} (V_n - V_{pcc})}{\frac{X_i + X_{vi}}{n_i} + V_{pcc}} \quad (11)$$

The well established condition for power sharing is given by

$$n_1 Q_1 = n_2 Q_2 = \dots = n_N Q_N \quad (12)$$

To satisfy (12), from (11) we get

$$\frac{X_1 + X_{v1}}{n_1} = \frac{X_2 + X_{v2}}{n_2} = \dots = \frac{X_N + X_{vN}}{n_N} \quad (13)$$

Satisfying both (12) and (13) the condition for proportionate sharing of reactive power is given as

$$Q_1 (X_1 + X_{v1}) = Q_2 (X_2 + X_{v2}) = \dots = Q_N (X_N + X_{vN}) \quad (14)$$

The  $X_{vi}$  value is updated to satisfy above condition.

## IV. CONSENSUS ALGORITHM AND VIRTUAL VOLTAGE DROP

### A. Graph Theory

The communication among the DGs can be realised using the graph theory. Graph with  $N$  nodes can be represented as  $G = (V_G, E_G, A_G)$ . Where  $V_G$  represents the nodes of the graph,  $E_G$  represents the edges and  $A_G$  represents the adjacency matrix. The communication links between DGs are represented by edges  $E_G$  and the information flow is represented by each edge pair.  $A_G$  conveys if there is information

flow or not among the two DGs represented by nodes in the graph. Two important matrices are in degree matrix, represented as  $D = \text{diag}\{d_i\} \in \mathbb{R}^{N \times N}$  and Laplacian matrix, defined as  $L_G = D - A_G$ .

### B. Adaptive virtual impedance control based on consensus algorithm

A complete block diagram of the proposed controller is shown in Fig. 2. The information about the local DGs reactive power-sharing is achieved by implementing the popularly used consensus algorithm as shown below

$$Q_{ierr} = \sum_{j=N_i} a_{ij} (n_i Q_i - n_j Q_j) \quad (15)$$

Where  $a_{ij}$  is the element of the adjacency matrix.  $Q_{ierr}$  represents the reactive power-sharing error from the neighbourhood DGs. A coupling gain value is multiplied with this

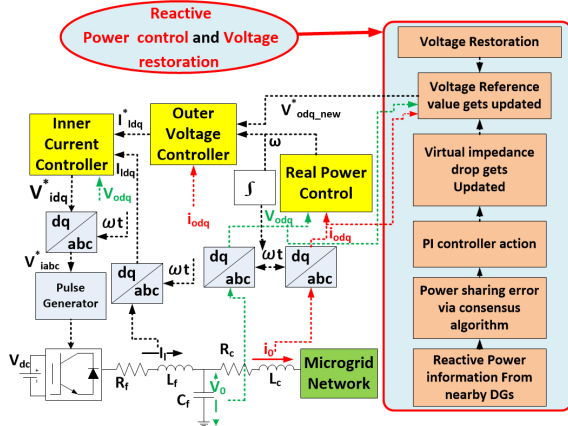


Fig. 2. Block diagram of the proposed controller.

reactive power sharing error term to obtain the reactive power mismatch term as given below

$$Q_{imis} = -K_{nQ}Q_{ierr} \quad (16)$$

The reactive power mismatch term is actuated by proportional-integral (PI) controller  $H_i(s)$  and a virtual impedance correction term is obtained as

$$\delta Q_{icorr} = H_i(s) Q_{imis} \quad (17)$$

The coupling gain and the PI controller gain value makes the system stable by establishing relationship between reactive power sharing error  $Q_{ierr}$  and the virtual impedance correction term  $\delta Q_{icorr}$ . This  $\delta Q_{icorr}$  term is scaled by scalar gain  $G_{QL}$  and negated from static inductance and resistance value to obtain the adaptive inductance and resistance values respectively as given by equations below.

$$L_{vi} = L_{vi}^* - G_{QL} \delta Q_{icorr} \quad (18)$$

$$R_{vi} = R_{vi}^* - G_{QR} \delta Q_{icorr} \quad (19)$$

### C. Virtual Drop

The virtual inductance and resistance introduces the virtual drop in the system as governed by the below given equations

$$v_{vi\_d} = I_{oi_d} R_{vi} - I_{oi_q} \omega L_{vi} \quad (20)$$

$$v_{vi\_q} = I_{oi_q} R_{vi} + I_{oi_d} \omega L_{vi} \quad (21)$$

Where  $R_{vi}$  and  $L_{vi}$  are the virtual resistance and the virtual inductance respectively. As this leads to drop in the average value of output voltages from DGs therefore a voltage restoration is implemented to elevate the average of output voltages from all the DGs to 230 V. The conventional droop equation gets modified after implementing the proposed controller. The new equation becomes

$$v_{od\_new}^* = V_n - nQ - v_{vi\_d} \quad (22)$$

$$v_{oq\_new}^* = 0 \quad (23)$$

$v_{og\_new}^*$  is still kept zero. This new reference value is given to voltage controller.

## V. SIMULATION AND RESULT DISCUSSION

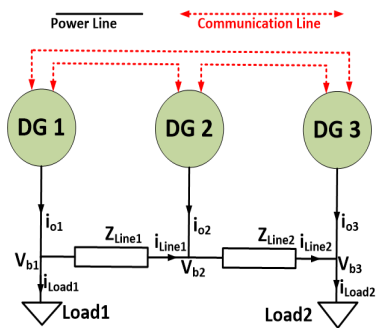


Fig. 3. Test network

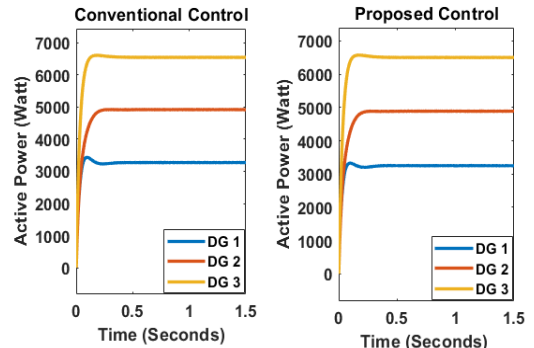


Fig. 4. Active Power sharing in conventional control and proposed control.

The proposed controller is implemented to a typical test network shown in Fig. 3. Here three DGs are connected in parallel to share the total demand (Load1 and Load2). The line impedances connecting the DGs to load sides are  $Z_{Line1}$  and  $Z_{Line2}$ . System and control parameters are given in table I. Simulation of the proposed controller and its validation through various case studies have been done in MATLAB.

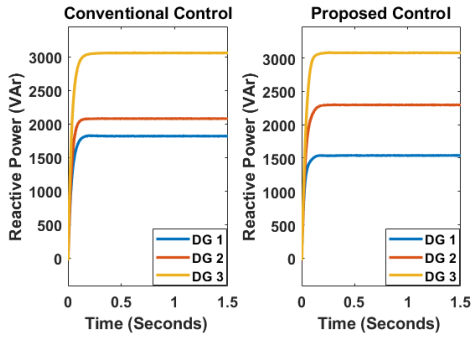


Fig. 5. Reactive Power sharing in conventional and proposed control.

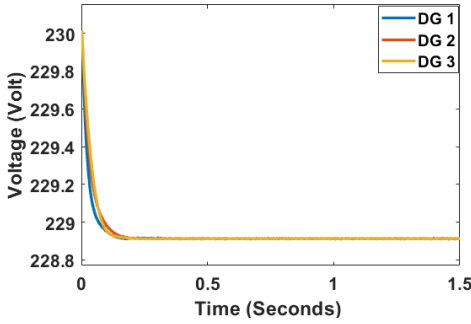


Fig. 6. Droop voltages in case of proposed control

TABLE I  
SYSTEM AND CONTROL PARAMETERS

Parameter	Value	Parameter	Value
$V_{dc}$	720 V	$V_n$	325.27 V
$L_f$	1.5 mH	$L_c$	0.50 mH
$R_f$	1.9Ω	$R_c$	0.08Ω
$C_f$	210μF	$\omega_c$	31.41 rad/s
$Z_{Line1}$	$(0.0175+j0.043)\Omega$	$Load1 (P+jQ)$	$5+j2$
$Z_{Line2}$	$(0.03+j0.132)\Omega$	$Load2 (P+jQ)$	$10+j5$
$m_1$	$2.18*10^{-5}$	$n_1$	$1*10^{-3}$
$m_2$	$1.45*10^{-5}$	$n_2$	$0.67*10^{-3}$
$m_3$	$1.09*10^{-5}$	$n_3$	$0.5*10^{-3}$
$K_nQ$	-7.5	$H_p$	0.02
$H_i$	10	$G_{QL}$	$1.5*10^{-4}$
$G_{QR}$	0.02	$K_E$	4
$C_p$	0.30	$C_i$	0.02
$L_v^*$	$0.5*10^{-3}$	$R_v^*$	$5*10^{-2}$
$F_{sw}$	10 kHz		

#### A. Case I. Conventional Droop vs. Proposed Control

The proposed controller is implemented in the test network given by Fig. 3. In terms of active power sharing the conventional control works fine as shown in Fig. 4 but while it comes to reactive power sharing the conventional control leads to improportionate power sharing as shown in left part of Fig. 5. With implementation of proposed controller, it can be seen that as the ratings of the DGs are in the ratio of 1:1.5:2, the reactive power is also shared proportionately in the ratio of 1:1.5:2. DG3 with highest power rating share highest amount of power among all the DGs. The droop voltage in case of conventional control do not achieve consensus

while in proposed control with time the droop output voltages become equal as shown in Fig. 6, leading to the proportionate sharing of reactive powers. Most of the earlier works on

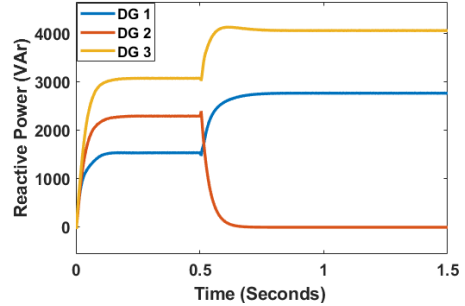


Fig. 7. Reactive power sharing while Unplugging DG2

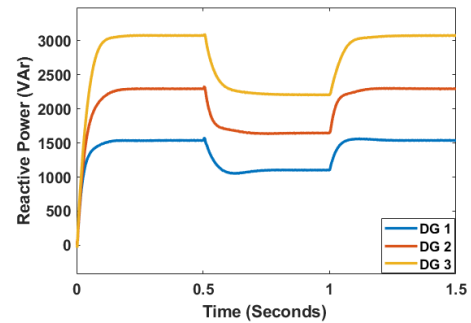


Fig. 8. Reactive power sharing during changing load conditions

consensus-based power sharing are done by considering static resistance or static value of reactance. This paper presents adaptive reactance and resistances-based control. The value of resistances and reactances are adaptively updated until the droop voltages becomes equal so as the reactive power is shared in proportion.

#### B. Case II. Unplugging one DG

At  $t = 0.5s$   $DG_2$  is plugged out from the system. The controller acts fine in this case also and from Fig.7 it can be seen that the reactive power sharing of the  $DG_2$  becomes zero after it is plugged out while the other two DGs raises their power sharing to meet the load demand. Meanwhile the droop voltage of  $2^{nd}$  DG increases while the droop voltage of  $DG_1$  and  $DG_3$  becomes equal leading to proportionate reactive power sharing. The system is stable even in such plugged out behavior which is quite important as DG outage may take place in a system or DGs may be intentionally removed for planned maintenance.

#### C. Case III. Changing value of loads

The controller proposed in this paper works well for the case of load variations too. At  $t = 0.5s$  load 1 is disconnected and is again connected back at  $t = 1s$ . It can be seen from Fig. 8 that with decrease in load the power sharing ratio is still maintained and with increase in load the power demand increases and also the power sharing ratio is maintained.

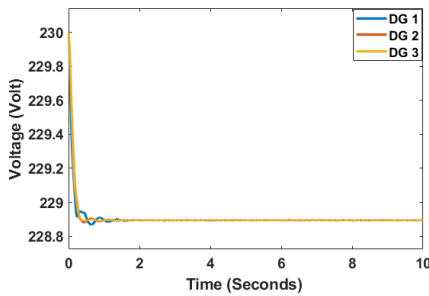


Fig. 9. Droop voltages for communication delay of 0.100s

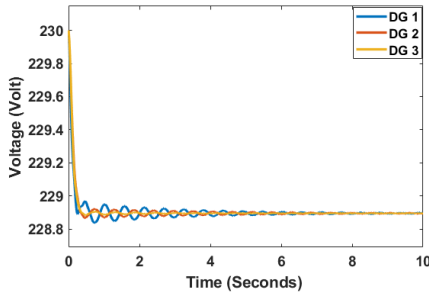


Fig. 10. Droop voltages for communication delay of 0.130s

#### D. Case IV. Restoring the voltage value

As the virtual drop tends to reduce the overall voltage, the voltage value is restored using voltage restoration technique. Here average consensus algorithm is used to restore the average value of voltages to 230 V as shown in Fig.12. The average consensus technique considering  $d$  component of output voltage  $V_{oi}$  as  $V_{odi}$  is given as:

$$\bar{V}_{oi}(t) = \bar{V}_{odi}(t) + K_E \int \sum_{j \in N_i} (V_{oj}(t) - \bar{V}_{oi}(t)) dt \quad (24)$$

This average output value is compared with  $V_n$  value and voltage mismatch is obtained

$$V_{oi_{miss}} = V_n - \bar{V}_{oi} \quad (25)$$

The PI controller gain  $C_P$  and  $C_I$  generates voltage correction term  $\delta V_{oi}$ . This voltage correction term modifies (22) to (27)

$$\delta V_{oi} = C_i(s) V_{oi_{miss}} \quad (26)$$

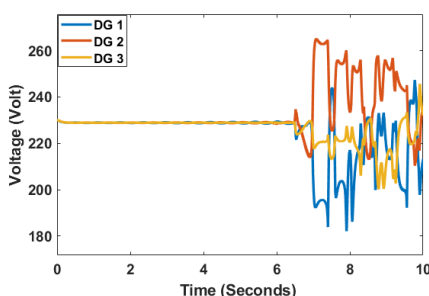


Fig. 11. Droop voltages for communication delay of 0.150s

$$v_{od\_new}^* = V_n - nQ - v_{vi\_d} + \delta V_{oi} \quad (27)$$

Since the local output values of each DGs are updated, the average value is also updated to the desired value of 230 V.

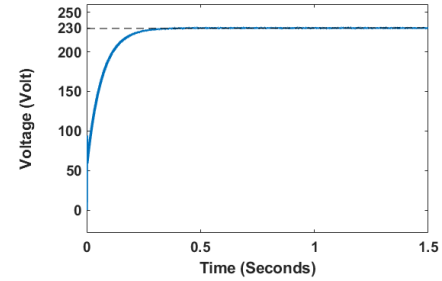


Fig. 12. Average output voltage for three DGs

#### E. Case V. Communication Delay

As secondary control of voltage restoration is applied it is very much essential to address the problem of communication delay. Communication delay beyond tolerable value may lead to instability in the system. It is found here in this proposed system the maximum tolerable value of communication delay is of 0.130s as shown in Fig.10. It can be seen from Fig. 9 that a time delay of less than 0.130s does not impact the system stability. For time delay value greater than 0.130s the system becomes unstable as shown in fig.11, where a delay of 0.150s lead to oscillatory drooped voltages eventually leading to instability.

#### VI. SMALL SIGNAL STABILITY ANALYSIS

Small signal stability analysis of the complete model is done to assess the system behavior under different operating parameters. A complete system matrix is obtained by modeling the individual components of the complete model. Unlike in previous work in modeling of inverter based microgrid [18], here the effect of the proposed virtual impedance controller is also addressed that can be seen from introduction of  $D_{pi}$  matrix in the power controller model which eventually modifies the  $A_{INV_i}$  matrix given in [18]. The modified matrix is given below, all the other matrices are same as the matrices given in [18].

$$A_{INV_i} = \begin{bmatrix} A_{Pi} & 0 & 0 & B_{Pi} \\ B_{V1i}C_{Pvi} & 0 & 0 & B_{V2i} + B_{V1i}D_{Pi} \\ B_{C1i}D_{V1i}C_{Pvi} & B_{C1i}C_{Vi} & 0 & B_{C1i}(D_{V1i}D_{Pi} + D_{V2i}) \\ B_{LCL1i}D_{C1i}D_{V1i}C_{Pvi} & B_{LCL1i}D_{C1i}C_{Vi} & B_{LCL1i}C_{ci} & A_{LCL1i} \\ +B_{LCL2i}[T_{Vi}^{-1} 0 0] & +B_{LCL3i}C_{Pwi} & +B_{LCL1i}(D_{C1i}D_{V1i}D_{Pi} \\ +D_{C1i}D_{V2i} + D_{C2i}) \end{bmatrix} \quad (28)$$

Where  $D_{Pi}$  is given by:

$$D_{Pi} = \begin{bmatrix} 0 & 0 & 0 & R_{vi} & -\omega L_{vi} & 0 \\ 0 & 0 & 0 & 0 & 0 & 0 \end{bmatrix} \quad (29)$$

Real part of all the obtained eigenvalues of the complete system matrix lies in the left half of the eigenvalues plot

as shown in Fig. 13 validating the stability of the proposed model. It has also been observed that even with variation in line impedance the real part of eigenvalues lies in the left half of the plot. This validates that the proposed controller works fine even in the case of line impedance mismatch. The fact that the values of virtual inductances has crucial role in terms of the stability of the system can be appreciated from the fig.14. The plot is zoomed out to see the effect of change in virtual inductance value. The  $L_{v1}$  and  $L_{v2}$  values are fixed and the  $L_{v3}$  value is varied in a range. The arrow in fig.14 indicates that with the increase in values of  $L_{v3}$  the modes of the system tends to move towards the instability.

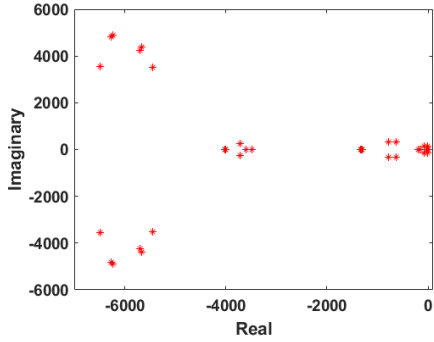


Fig. 13. Eigenvalues plot of system matrix for the proposed controller

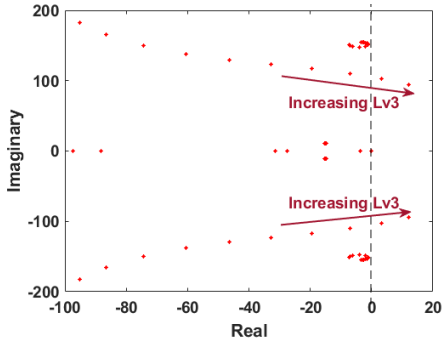


Fig. 14. Eigenvalues for  $L_{v1}=0.55$  mH,  $L_{v2}=0.35$  mH with varying  $L_{v3}$

## VII. CONCLUSION

This paper proposes a consensus-based adaptive virtual impedance control method for the proportionate reactive power-sharing among the parallel connected DGs in an islanded microgrid. The droop coefficients of the proposed controller are inversely proportional to the power values, which can be achieved by adjusting the dynamic component of virtual impedance. In this paper for the selected droop values of  $n1 = 1 * 10^{-3}$ ,  $n2 = 0.67 * 10^{-3}$  and  $n3 = 0.5 * 10^{-3}$ , the adaptive values of virtual inductances associated with different cases (unplugging one DG, changing value of loads, restoring the voltage value and communication delay) are in the range of  $(0.157 - 1.089)$  mH. Similarly, the value of virtual resistances lies in  $(3.88 - 128.9)$  mΩ. The voltage restoration technique is applied to restore the average voltage of all the DGs to 230

V. The robustness of the proposed controller is demonstrated through various case studies. Further, a small signal stability analysis is carried out to validate the stability of the test system. Also, the virtual inductance value is varied in a range of values to appreciate their impact on system stability.

## REFERENCES

- [1] H. Farhangi, "The path of the smart grid," in IEEE Power and Energy Magazine, vol. 8, no. 1, pp. 18-28, January-February 2010
- [2] M. H. Saeed, W. Fangzong, B. A. Kalwar and S. Iqbal, "A Review on Microgrids' Challenges Perspectives," in IEEE Access, vol. 9, pp. 166502-166517, 2021
- [3] X. Wu, Y. Xu, J. He, X. Wang, J. C. Vasquez and J. M. Guerrero, "Pinning-Based Hierarchical and Distributed Cooperative Control for AC Microgrid Clusters," in IEEE Transactions on Power Electronics, vol. 35, no. 9, pp. 9865-9885, Sept. 2020
- [4] J. M. Guerrero, M. Chandorkar, T. -L. Lee and P. C. Loh, "Advanced Control Architectures for Intelligent Microgrids—Part I: Decentralized and Hierarchical Control," in IEEE Transactions on Industrial Electronics, vol. 60, no. 4, pp. 1254-1262, April 2013
- [5] Z. Li, C. Zang, P. Zeng, H. Yu and S. Li, "Fully Distributed Hierarchical Control of Parallel Grid-Supporting Inverters in Islanded AC Microgrids," in IEEE Transactions on Industrial Informatics, vol. 14, no. 2, pp. 679-690, Feb. 2018
- [6] M. S. Golsorkhi and D. D. C. Lu, "A Control Method for Inverter-Based Islanded Microgrids Based on V-I Droop Characteristics," in IEEE Transactions on Power Delivery, vol. 30, no. 3, pp. 1196-1204, June 2015
- [7] L. Zhang, H. Zheng, Q. Hu, B. Su and L. Lyu, "An Adaptive Droop Control Strategy for Islanded Microgrid Based on Improved Particle Swarm Optimization," in IEEE Access, vol. 8, pp. 3579-3593, 2020
- [8] M. K. Behera and L. C. Saikia, "An Improved Voltage and Frequency Control for Islanded Microgrid Using BPF Based Droop Control and Optimal Third Harmonic Injection PWM Scheme," in IEEE Transactions on Industry Applications, vol. 58, no. 2, pp. 2483-2496, March-April 2022
- [9] M. C. Chandorkar, D. M. Divan and B. Banerjee, "Control of distributed UPS systems," Proceedings of 1994 Power Electronics Specialist Conference - PESC'94, Taipei, Taiwan, 1994
- [10] A. Bidram and A. Davoudi, "Hierarchical Structure of Microgrids Control System," in IEEE Transactions on Smart Grid, vol. 3, no. 4, pp. 1963-1976, Dec. 2012
- [11] M. Savaghebi, A. Jalilian, J. C. Vasquez and J. M. Guerrero, "Secondary Control Scheme for Voltage Unbalance Compensation in an Islanded Droop-Controlled Microgrid," in IEEE Transactions on Smart Grid, vol. 3, no. 2, pp. 797-807, June 2012
- [12] L. Li, Y. Sun, Z. Liu, X. Hou, G. Shi and M. Su, "A Decentralized Control With Unique Equilibrium Point for Cascaded-Type Microgrid," in IEEE Transactions on Sustainable Energy, vol. 10, no. 1, pp. 324-326, Jan. 2019
- [13] G. Shi, H. Han, Y. Sun, J. Ou, Y. Guan and J. M. Guerrero, "A Decentralized Secondary Frequency Restoration Control With Local Current for Island Cascaded-Type Microgrids," in IEEE Transactions on Power Systems, vol. 38, no. 4, pp. 3136-3146, July 2023
- [14] X. Yan, Y. Zhang, W. Zhang and J. Tang, "Circulating-current analysis and power sharing control of parallel inverters with different capacities," International Conference on Renewable Power Generation (RPG 2015), Beijing, 2015
- [15] P. Sreekumar and V. Khadkikar, "A New Virtual Harmonic Impedance Scheme for Harmonic Power Sharing in an Islanded Microgrid," in IEEE Transactions on Power Delivery, vol. 31, no. 3, pp. 936-945, June 2016
- [16] Y. Gu, W. Li and X. He, "Frequency-Coordinator Virtual Impedance for Autonomous Power Management of DC Microgrid," in IEEE Transactions on Power Electronics, vol. 30, no. 4, pp. 2328-2337, April 2015
- [17] Y. C. C. Wong, C. S. Lim, A. Cruden, M. D. Rotaru and P. K. Ray, "A Consensus-Based Adaptive Virtual Output Impedance Control Scheme for Reactive Power Sharing in Radial Microgrids," in IEEE Transactions on Industry Applications, vol. 57, no. 1, pp. 784-794, Jan.-Feb. 2021
- [18] N. Pogaku, M. Prodanovic and T. C. Green, "Modeling, Analysis and Testing of Autonomous Operation of an Inverter-Based Microgrid," in IEEE Transactions on Power Electronics, vol. 22, no. 2, pp. 613-625, March 2007